

## Cu- and Yb- based planar triangular lattice magnets: from gapless spin liquids, spin orbit entanglement and field induced magnetic order

Michael Baenitz<sup>#</sup>, Burkhard Schmidt<sup>##</sup>, Kizhake M. Ranjith, Helge Rosner, Seunghyun Khim, Kimberly Modic, Jörg Sichelschmidt, Marcus Schmidt, Dmitry Sokolov, Hiroshi Yasuoka

Spin 1/2 quantum magnetism has been extended away from 3d ions (like Cu<sup>2+</sup>- or V<sup>4+</sup>-ions) towards 4d-, 5d- and even 4f-systems [1]. Here an effective  $j_{\text{eff}} = 1/2$  moment can be realized due to the presence of strong spin-orbit coupling (SOC). The strong impact of the spin-orbit entanglement in general and the bond dependent exchange frustration in particular has become evident in recent years and has significantly boosted the search for new spin liquid systems. Especially Yb-based magnets moved into the center of interest and the triangular lattice magnet (TLM) NaYbS<sub>2</sub> seems to be a prime candidate for this new type of quantum spin liquid (QSL) [2, 3]. Understanding the SOC driven QSLs is rather challenging and goes far beyond Andersons RVB theory [4]. In contrast to YbMgGaO<sub>4</sub>, which shares the same space group (R-3m) and was highlighted as the first SOC-TLM-QSL, NaYbS<sub>2</sub> as a unique model system lacks inherent lattice distortions and Yb resides on a centrosymmetric position in the YbS<sub>6</sub> octahedron [2]. We were able to identify the entire new series of Yb-delafoffsites NaYbCh<sub>2</sub> as a new class of spin orbit entangled TLM and gapless QSL-s hosted on a perfect triangular lattice [2, 5, 6]. The magnetic exchange is rather anisotropic and the application of magnetic fields within the (a,b)-plane first suppresses the generic critical fluctuations and tunes the QSL towards a magnetic ordered states. In contrast to that for fields in the c-direction the system remains relatively robust and stays paramagnetic.

Two-dimensional (2D) planar spin arrangements on complex patterns like the Kagome- type or honeycomb type favor the evolution of a spin liquid ground state out of the paramagnetic gas towards low temperatures. However, the simplest geometry, the 2D-triangular lattice, was highlighted almost 50 years ago by P. Anderson [4] as a host for spin liquids.

For this reason, we have continued to work on Cu-based triangular lattice systems. Here, we unveil a new stoichiometric spin liquid candidate Sr<sub>3</sub>CuSb<sub>2</sub>O<sub>9</sub> [7] and present the inherently diluted system Y<sub>2</sub>CuTiO<sub>6</sub> where Cu<sup>2+</sup> - and Ti<sup>4+</sup> - ions share the same lattice site in a 50:50 proportionality in corner-shared (Cu/Ti)O<sub>5</sub> polyhedra and the evolution of a disorder driven QSL is discussed [8].

The Kramers ions among the 4f ions (f.i. Yb and Ce) can exhibit a pronounced ground-state doublet with an effective spin of 1/2 which is formed due to crystal electric fields of low symmetry.

Here for TLMs the spin-orbit entanglement can lead to highly anisotropic bond-dependent interactions among the moments, which strongly enhance quantum fluctuations and promote a QSL ground state [9]. A consequence is that off diagonal terms in the exchange matrix in the xxz Heisenberg type exchange model became important and can dominate the exchange at small magnetic fields, leading (together with anisotropic quantum fluctuations) to the suppression of long range order and the evolution of a QSL [10].

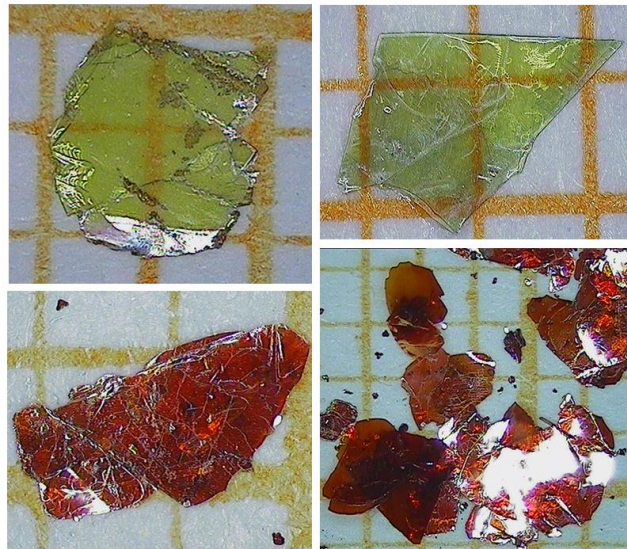


Fig. 1: Examples of plate - like NaYbS<sub>2</sub> (top row) and NaYbSe<sub>2</sub> (bottom row) single crystals used for our studies. The growth of the crystals is such that the lateral dimension corresponds to the (a,b)-plane while perpendicular to it the c-direction of the rhombohedral structure is found.

In contrast to that, in the absence of SOC, the classical  $S = 1/2$  isotropic Heisenberg model (with isotropic nearest neighbor interaction nn) predicts the energy-minimum solution to be the planar 120° Néel-ordered state with a strong magnetic anisotropy. An additional next-nearest-neighbor interaction (nnn) can quench the 120° order and drive the system also towards a QSL or an antiferromagnetic stripe phase [11, 12].

As already mentioned in the last report, we were triggered by the huge interest on the  $4f$ -triangular magnet QSL candidate  $\text{YbMgGaO}_4$  [13] and focused our efforts on new Yb-quantum magnets within the same space group ( $R\bar{3}m$ ). We now succeeded to show that the delafossite type series  $\text{NaYbCh}_2$  ( $\text{Ch} = \text{O}, \text{S}, \text{and Se}$ ) provide a unique platform to study the field-induced crossover from an emerging spin-orbit-driven QSL at low fields to an isotropic two-dimensional (2D) planar spin-1/2 TLAf with particular types of planar long range magnetic order at much higher fields [2, 5, 6].

We were able to synthesize polycrystalline  $\text{NaYbO}_2$  and  $\text{AgYbO}_2$  at the MPI by solid-state reaction [5].  $\text{NaYbS}_2$  and  $\text{NaYbSe}_2$  plate-like single crystals were grown by a modified method following Lissner and Schleid [2, 6], starting from rare-earth metal grains of sulfur and selenium, and with sodium chloride as the flux (Fig. 1). This was done at the university in Dresden in the frame of the Collaborative Research Center SFB 1143 from the German Science Foundation (DFG). Our comprehensive approach combines bulk methods (susceptibility, high field magnetization, specific heat), local probes (electron spin resonance (ESR) [5, 6, 14, 15], nuclear magnetic resonance (NMR) [2, 5, 6, 16], muon spin relaxation ( $\mu\text{SR}$ ) [2, 17]) and complex exchange calculations.

As shown in Fig. 2, the crystal structure is composed of edge-shared  $\text{YbCh}_6$  and  $\text{NaCh}_6$  octahedra. The  $\text{YbCh}_6$  octahedra are weakly distorted and tilted along the Yb-Yb bond by an angle of  $53.33^\circ$  for  $\text{NaYbSe}_2$ ,  $\approx 48.60^\circ$  for  $\text{NaYbS}_2$  and  $47.70^\circ$  for  $\text{NaYbO}_2$ . The tilting angle for an undistorted octahedron is  $\alpha \sim 54.74^\circ$ . The local spin anisotropy (determined by the CEF splitting) as well the exchange anisotropy (given by the complex super exchange via the chalcogenide  $p$ -states) depends strongly on the octahedral tilt.

Above 80 K the Curie-Weiss fit gives a Weiss temperature of  $-66$  K and an effective moment  $\mu_{\text{eff}} = 4.5\mu_{\text{B}}$  which is in agreement with the free ion value of  $4.54\mu_{\text{B}}$  for  $j=7/2$  (Fig 3 (a)). Below 80 K the  $j_{\text{eff}}=1/2$  state evolves. After subtracting the Van - Vleck contribution (obtained from high field measurements Fig 3 (b)) the susceptibility  $\chi(T)$  for  $2\text{ K} < T < 30\text{ K}$  could be fitted with a Curie-Weiss law (inset Fig. 3(a)), which yields a Weiss temperature of  $-7$  K, and an effective moment of  $\mu_{\text{eff}} \approx 2.43\mu_{\text{B}}$  and a Weiss temperature of  $-3.5$  K and a moment of  $\mu_{\text{eff}} \approx 1.1\mu_{\text{B}}$  for the fields in the  $ab$ - plane and in the  $c$ - direction, respectively. These low-T CW moments are consistent

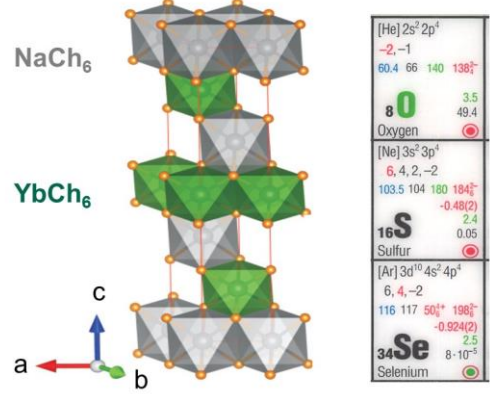


Fig. 2: Lattice structure of the Yb- delafossite series  $\text{NaYbCh}_2$  (left) and section of the chalcogenide from the periodic table (right). An increase of the ionic radii for the  $-2$  oxidation state from oxygen to selenium (via sulfur) and the variation of the  $\text{Ch-}p$  states involved in the super exchange is evident.

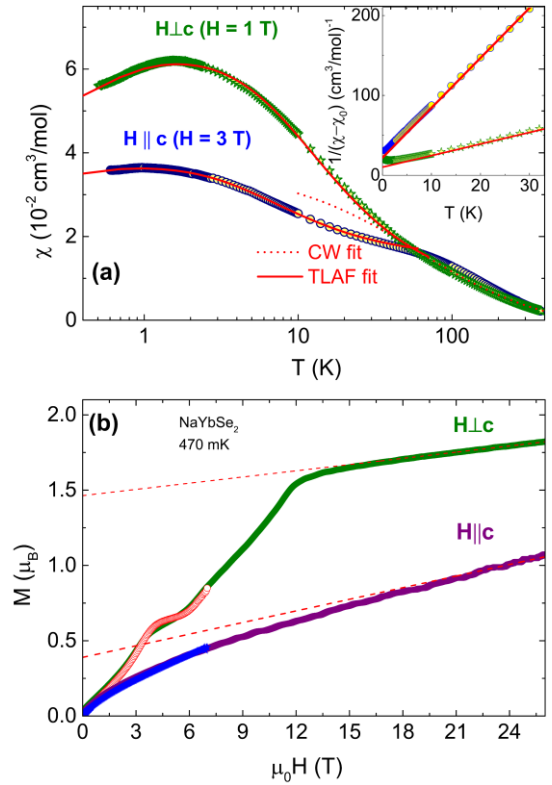


Fig. 3: (a) Magnetic susceptibilities of  $\text{NaYbSe}_2$  single crystals for  $H \perp c$  and  $H \parallel c$ . Red dotted and solid lines correspond to the high-temperature Curie-Weiss (CW) and triangular lattice approximation fittings, respectively. The inset shows the low-T inverse susceptibility after subtracting the Van Vleck contribution along with the CW fit for both directions. (b) Isothermal magnetization  $M(H)$  measured at 470 mK for both directions. Dashed lines represent the Van Vleck contribution [6].

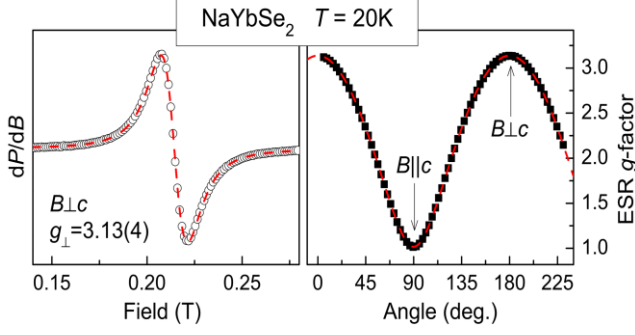


Fig. 4: Typical ESR-spectrum (left) and  $g$ -factor anisotropy (right) of a  $\text{NaYbSe}_2$  single crystal. Dashed lines denote data fittings with a Lorentzian spectrum shape and a uniaxial  $g$ -factor dependence on the angle between  $B$  and  $c$ -axis, respectively [6, 15].

with the measured  $g$ -values from the ESR (Fig. 4) within the  $j_{\text{eff}} = 1/2$  pseudospin model. The same is true for the saturation moments obtained from the high field measurements. The pronounced maximum in the susceptibility (Fig. 3(a)) corresponds to the maximum in the specific heat (Fig. 5(a)) and is a unique hallmark of low dimensional spin systems [12]. The pseudospin model is discussed in detail in the last section.

For the  $H \perp c$  direction, a field-induced phase transition is observed in the specific heat (Fig. 5 (b)) and also in  $M(H)$  indicated by a kink at  $1/3$  of the saturation magnetization ( $M_{1/3} \approx 0.6 \mu_B$ , Fig 3 (b)). For the  $H \parallel c$  direction, a field-induced transition is found for  $\text{NaYbSe}_2$  at much higher fields (Fig. 6) whereas it is absent ( $< 50$  T) for  $\text{NaYbS}_2$ . Upon the application of fields the QSL ground state is quenched and for  $H \perp c$  the systems converts into a more classical planar triangular spin  $1/2$  system with successive crossover

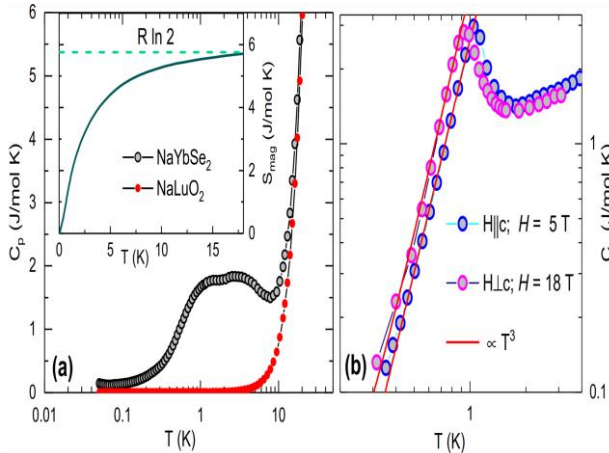


Fig. 5: (a) Specific heat of  $\text{NaYbSe}_2$  together with the nonmagnetic reference  $\text{NaLuO}_2$  in zero field as a function of temperature. The inset shows the entropy  $S(T)$ . (b) Field induced order as evidenced by a peak in  $C(T)$  for selected fields and orientations [6].

transitions from  $120^\circ$  Néel-ordered state to up-up-down state (uud) and to canted uud-variants and finally to the field polarized state (Fig. 6).

At the moment, investigations on the dilute system  $\text{Na}(\text{Yb},\text{Lu})\text{S}_2$  are in progress. Here the question is at which doping the liquid state changes into a gaseous i.e. single ion paramagnet. Furthermore, we investigate  $\text{NaGdS}_2$ . Here the SOC does not play a role, but magnetic ordering is also absent. Another interesting aspect is the fact that the triangular delafossite lattice can be transformed into the honeycomb lattice. We replaced the trivalent ion (e.g. Co) by a monovalent ion (e.g. Li) and a tetravalent magnetic ion (Ir) in a ratio of 1:2. Thus  $\text{PdCoO}_2$  is transferred to  $\text{Pd}_3\text{LiIr}_2\text{O}_6$ . Here, the 2D conductivity of  $\text{PdCoO}_2$  is coupled with the magnetic frustration in the honeycomb Ir lattice, which suggests unusual properties. In addition, we plan to investigate non Kramer ion systems like  $\text{NaTmO}_2$  where a Kosterlitz-Thouless melting of magnetic order is discussed. Another activity is in the direction of semi-metallic non-oxy delafossites with Cr (e.g.  $\text{AgCrSe}_2$ ) where chiral magnetism occurs due to symmetry reduction.

### Tuned Kagome – minerals and $\text{RuCl}_3$ : proximate QSLs with a triangle motif

Herbertsmithite  $\text{ZnCu}_3(\text{OH})_6\text{Cl}_2$  is a mineral and prototype QSL. Based on this material, we launched two initiatives. On the one hand, we tried to dope herbertsmithite by replacing  $\text{Zn}^{2+}$  by  $\text{Ga}^{3+}$  [18]. Here metalllicity and superconductivity was predicted [19]. On the other hand, we synthesized the mineral Barlowite  $\text{Cu}_4(\text{OH})_6\text{FBr}$  [20, 21] which is a polymorph of Herbertsmithite. Both systems are investigated by the local NMR probe ( $^{69,71}\text{Ga}$ - &  $^{79,81}\text{Br}$ - NMR) and unconventional magnetic order at the verge a QSL state is evidenced. Furthermore, it was shown that the Mott state of the minerals in general is rather robust against doping and the additional charge is shifted into hydrogen bonds. For the  $\text{RuCl}_3$  system, the magnetic anisotropy has been studied in detail using new novel methods such as resonant torsion magnetometry [21, 22].

### Hamiltonian, pseudospin exchange and magnetization

For the description of our experiments, we use a model Hamiltonian for  $\nu$   $\text{Yb}^{3+}$  ions of the form

$$\mathcal{H} = \sum_{i=1}^{\nu} [\mathcal{H}_{\text{CEF}}(i) + \mathcal{H}_{\text{Zeeman}}(i) + \mathcal{H}_{\text{exc}}(i)], \quad (1)$$

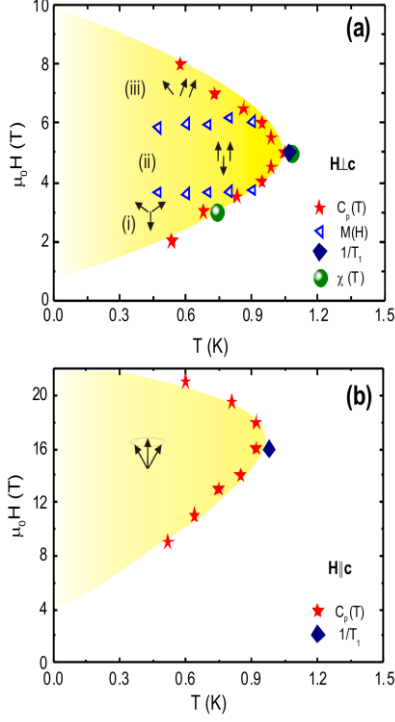


Fig. 6: Field-temperature phase diagram of NaYbSe<sub>2</sub> for H Lc (a) and H II c (b) [6].

comprised of a crystal field potential, a Zeeman coupling to an applied magnetic field, and an exchange between neighboring Yb<sup>3+</sup> ions. Here,  $H_{\text{CEF}}(i)$  is the trigonal crystal-field Hamiltonian at site  $i$ , splitting the eight  $j=7/2$  states into four doublets.  $H_{\text{CEF}}$  couples  $|j=7/2, m\rangle$  states with  $\Delta m=\pm 3$ , such that three of the four doublets have the form

$$|\psi^\pm\rangle = \mp\alpha e^{\pm i\phi_\alpha} \left| \frac{7}{2}, \pm \frac{7}{2} \right\rangle + \beta \left| \frac{7}{2}, \pm \frac{1}{2} \right\rangle \pm \gamma e^{\mp i\phi_\gamma} \left| \frac{7}{2}, \mp \frac{5}{2} \right\rangle \quad (2)$$

where  $\alpha$ ,  $\beta$ , and  $\gamma$  are real with  $\alpha^2 + \beta^2 + \gamma^2 = 1$  and  $\phi_\alpha = \phi_\gamma + 2\pi n$ ,  $n$  integer. The fourth doublet is the pure state  $|7/2, \pm 3/2\rangle$ . One of the three doublets in Eq. (2) is the ground state which we map onto a pseudospin by defining g factors

$$g_{\parallel} := g_j (7\alpha^2 + \beta^2 - 5\gamma^2), \quad (3)$$

$$g_{\perp} := g_j (2\sqrt{7}\alpha\gamma + 4\beta^2)$$

with  $g_j = 8/7 \approx 1.14$  (Landé factor). In an applied magnetic field  $\mathbf{B} = \mu_0 \mathbf{H}$ , the Zeeman Hamiltonian is then given by

$$\mathcal{H}_{\text{Zeeman}}(i) = -\mu_0 g_j \mu_B \sum_{\alpha} J_i^{\alpha} H_{\alpha}$$

$$\rightarrow -\mu_0 \mu_B [g_{\parallel} S_i^z H_z + g_{\perp} (S_i^x H_x + S_i^y H_y)], \quad (4)$$

where  $\mu_0$  is the magnetic permeability constant and  $\mu_B$  the Bohr magneton.

Finally, the exchange interaction between neighboring Yb<sup>3+</sup> pseudospins for an arbitrary but fixed site  $i$  can be written as

$$\mathcal{H}_{\text{exc}}(i) = \frac{1}{2} \sum_{\langle ij \rangle} \sum_{\alpha\beta} J_i^{\alpha} \hat{J}_{ij}^{\alpha\beta} J_j^{\beta}$$

$$\rightarrow \frac{1}{2} \sum_{\langle ij \rangle} \sum_{\alpha\beta} S_i^{\alpha} J_{ij}^{\alpha\beta} S_j^{\beta} \quad (5)$$

where the sum is taken over the  $z=6$  bonds connecting sites  $j$  and site  $i$  with an exchange tensor  $J$  (not to be confused with total moment  $J$ ) having the respective components  $J^{\alpha\beta}_{ij}$ . Defining the Cartesian  $x$  direction parallel to one Yb–Yb bond, the  $z$  direction perpendicular to the triangular - lattice plane (parallel to the crystallographic  $c$  direction), the local site symmetry tells us that the exchange along that particular bond has the form

$$J_{ij} = \begin{pmatrix} J_{\perp} & 0 & 0 \\ 0 & J_{\perp} & 0 \\ 0 & 0 & J_{\parallel} \end{pmatrix} + \begin{pmatrix} J_{\Delta} & 0 & 0 \\ 0 & -J_{\Delta} & J_{yz} \\ 0 & J_{yz} & 0 \end{pmatrix} \quad (6)$$

Here we have split  $J_{ij}$  into a part rotationally invariant around the  $c$  direction plus a traceless part depending on the bond direction. We note that only due to the trigonal distortion of the YbO<sub>6</sub> quasi-octahedra the latter can be finite. An expression for the full pseudospin exchange Hamiltonian can be found in Ref. [6].

The dimensionless uniform magnetic susceptibility  $\chi(T)$  of a crystal with volume  $V$  is given by the change of the magnetisation  $M$  with the magnetic field  $\mathbf{B} = \mu_0 \mathbf{H}$  with components

$$\chi_{\alpha} := \mu_0 \frac{\partial M_{\alpha}}{\partial B_{\alpha}} = \frac{\mu_0}{V} \frac{\partial \bar{\mu}_{\alpha}}{\partial B_{\alpha}} = -\frac{\mu_0}{V} \frac{\partial^2 F}{\partial B_{\alpha}^2}, \quad \alpha = \parallel, \perp \quad (7)$$

Where  $\mu_{\alpha} = -\partial F / \partial B_{\alpha}$  is the total magnetic moment in spatial direction  $\alpha$  either parallel or perpendicular to the  $c$  axis and  $F = (1/\beta) \log Z$  the canonical free energy,  $1/\beta = k_B T$  the inverse temperature and  $k_B$  the Boltzmann constant. For the molar susceptibility, multiply Eq. (7) with  $N_L / (v/V)$  where  $N_L$  is Avogadro's number and  $v/V$  the volume density of Yb<sup>3+</sup> ions.

A high-temperature expansion of Eq. (7) for temperatures  $T \gg |B_{\perp}^0 / k_B|, |J_{\parallel, \perp} / k_B|$  gives in the limit  $\beta \rightarrow 0$  a Curie Weiss law

$$\hat{\chi}_{\alpha} = \frac{\nu}{V} \frac{\mu_0 \hat{\mu}^2}{3} \beta \left( 1 + \beta k_B \hat{\Theta}_{\alpha} \right) + \mathcal{O}(\beta^3), \quad (8)$$

with the full  $j = 7/2$  magnetic moment  $\mu = \mu_B g_j \sqrt{j(j+1)}$  per  $\text{Yb}^{3+}$ , and the Curie-Weiss temperatures

$$\begin{aligned} k_B \hat{\Theta}_{\parallel} &= -\frac{4}{5} \left( j - \frac{1}{2} \right) \left( j + \frac{3}{2} \right) B_2^0 \\ &\quad - \frac{j(j+1)}{3} \left( \frac{g_j}{g_{\parallel}} \right)^2 z J_{\parallel}, \\ k_B \hat{\Theta}_{\perp} &= +\frac{2}{5} \left( j - \frac{1}{2} \right) \left( j + \frac{3}{2} \right) B_2^0 \\ &\quad - \frac{j(j+1)}{3} \left( \frac{g_j}{g_{\perp}} \right)^2 z J_{\perp}. \end{aligned} \quad (9)$$

At temperatures  $T \gg |J_{\parallel, \perp}/k_B|$  but low enough such that only the ground-state doublet is thermally populated, we can derive a similar expression for  $\chi(T)$ ,

$$\chi_{\alpha} = \frac{\nu}{V} \frac{\mu_0 \mu_{\alpha}^2}{3} \beta (1 + \beta k_B \Theta_{\alpha}) + \mathcal{O}(\beta^3) \quad (10)$$

now with the  $s = 1/2$  pseudospin moments  $\mu_{\parallel, \perp} = \mu_B g_{\parallel, \perp} \sqrt{s(s+1)}$  per  $\text{Yb}^{3+}$ . Here the respective Curie-Weiss temperatures  $\Theta_{\parallel, \perp}$  parallel and perpendicular to the  $c$  direction are given by

$$k_B \Theta_{\parallel, \perp} = -\frac{s(s+1)}{3} z J_{\parallel, \perp} = -\frac{3}{2} J_{\parallel, \perp}. \quad (11)$$

The saturation field  $H_{\text{sat}}$ , defined as an instability of the fully field-polarized state towards  $\Delta m_s = 1$  spin flips, can be calculated within a classical approximation [6]. We regard the pseudospins as classical vectors living on a three-sublattice structure. On each sublattice any two spins are aligned parallel relative to each other. With a field parallel to the  $c$  direction, near saturation an umbrella-like arrangement of the sublattice moments around the field axis is the structure minimizing the classical energy density per spin. From this, we obtain

$$\mu_0 H_{\text{sat}}^{\parallel} = \frac{3s^2(2J_{\parallel} + J_{\perp})}{M_{\text{sat}}^{\parallel}} \quad (12)$$

for the saturation field with the saturation magnetization  $M_{\text{sat}}^{\parallel} = s g_{\parallel} \mu_B / \text{Yb}^{3+}$ . For a field in the triangular-lattice plane perpendicular to the  $c$  axis, a coplanar structure turns out to minimize the classical energy density per spin. In our case, infinitesimally below  $H_{\text{sat}}^{\perp}$  all three sublattice moments lie in the  $ab$  plane, and we obtain

$$\mu_0 H_{\text{sat}}^{\perp} = \frac{9s^2 J_{\perp}}{M_{\text{sat}}^{\perp}} \quad (13)$$

for the saturation field with  $M_{\text{sat}}^{\perp} = s g_{\perp} \mu_B / \text{Yb}^{3+}$ .

## External Cooperation Partners

Th. Doert (Technical University Dresden (TUD), Germany); D. Inosov (TUD, Germany); M. Itho (Nagoya University, Japan); K. Kanoda (University Tokyo, Japan); C. Krellner (Goethe University Frankfurt, Germany); H. Kühne (High field Laboratory, Rossendorf); A.V. Mahajan (Indian Institute of Technology, Bombay, India); P. Mendels (Université Paris-Saclay, France); K. Miyagawa (University Tokyo, Japan); B. J. Ramshaw (Cornell University, USA); A. Shekhter (Florida State University, USA); A. Strydom (University of Johannesburg, South Africa); D. D. Sarma (Indian Institute of Science, Bengaluru, India); A. Tsirlin (Augsburg University, Germany); J. Wosnitza (High field Laboratory Rossendorf & Technical University Dresden, Germany).

## References

- [1] *Spin liquids in frustrated magnets*, L. Balents, *Nature* **464** (2010) 199.
- [2]\* *NaYbS<sub>2</sub>: A planar spin-1/2 triangular-lattice magnet and putative spin liquid*, M. Baenitz, Ph. Schlender, J. Sichelschmidt, Y. A. Onyikienko, Z. Zangeneh, K. M. Ranjith, R. Sarkar, L. Hozoi, H. C. Walker, J.-C. Orain, et al., *Phys. Rev. B* **98** (2018) 220409(R).
- [3] *Rare-earth chalcogenides: A large family of triangular lattice spin liquid candidates*, W. Liu, Z. Zhang, J. Ji, Y. Liu, J. Li, X. Wang, H. Lei, G. Chen, and Q. Zhang, *Chin. Phys. Lett.* **35** (2018) 117501.
- [4] *Resonating valence bonds: A new kind of insulator?* P. W. Anderson, *Mater. Res. Bull.* **8** (1973) 153.
- [5]\* *Field-induced instability of the quantum spin liquid ground state in the Jeff = 1/2 triangular-lattice compound NaYbO<sub>2</sub>*, K. M. Ranjith, D. Dmytriieva, S. Khim, J. Sichelschmidt, S. Luther, D. Ehlers, H. Yasuoka, J. Wosnitza, A. A. Tsirlin, H. Kühne, and M. Baenitz, *Phys. Rev. B* **99** (2019) 180401(R).
- [6]\* *Anisotropic field-induced ordering in the triangular-lattice quantum spin liquid NaYbSe<sub>2</sub>*, K. M. Ranjith, S. Luther, T. Reimann, B. Schmidt, Ph. Schlender, J. Sichelschmidt, H. Yasuoka, A. M. Strydom, Y. Skourski, J. Wosnitza, et al., *Phys. Phys. Rev. B* **100** (2019) 224417.
- [7]\* *Gapless Quantum Spin Liquid in the Triangular System Sr<sub>3</sub>CuSb<sub>2</sub>O<sub>9</sub>*, S. Kundu, A. Shahee, A. Chakraborty, K. M. Ranjith, B. Koo, J. Sichelschmidt, M. T. F. Telling, P. K. Biswas, M. Baenitz, I. Dasgupta, et al., *Phys. Rev. Lett.* **125** (2020) 267202.
- [8]\* *Signatures of a Spin-1/2 Cooperative Paramagnet in the Diluted Triangular Lattice of Y<sub>2</sub>CuTiO<sub>6</sub>*, S. Kundu, A. Hossain, P. Keerthi, S. R. Das, M. Baenitz, P. J. Baker, J. C. Orain, D. C. Joshi, R. Mathieu, P. Mahadevan, et al., *Phys. Rev. Lett.* **125** (2020) 117206.

- [9] *Anisotropic spin model of strong spin-orbit-coupled triangular antiferromagnets*, Y.-D. Li, X. Wang, and G. Chen, *Phys. Rev. B* **94** (2016) 035107.
- [10] *Anisotropic-Exchange Magnets on a Triangular Lattice: Spin, Waves, Accidental Degeneracies, and Dual Spin Liquids* P. A. Maksimov, Z. Zhu, S. R. White, and A. L. Chernyshev, *Phys. Rev. X* **9** (2019) 021017.
- [11] *Quantum theory of an antiferromagnet on a triangular lattice in a magnetic field*, A. V. Chubukov and D. I. Golosov, *J. Phys.: Condens. Matter* **3** (1991) 69.
- [12] *Frustrated two dimensional quantum magnets*, B. Schmidt and P. Thalmeier, *Phys. Rep.* **703** (2017) 1.
- [13] *Rare-Earth Triangular Lattice Spin Liquid: A Single-Crystal Study of YbMgGaO<sub>4</sub>*, Y. Li, G. Chen, W. Tong, L. Pi, J. Liu, Z. Yang, X. Wang, and Q. Zhang, *Phys. Rev. Lett.* **115** (2015) 167203.
- [14]\* *Electron spin resonance on the spin-1/2 triangular magnet NaYbS<sub>2</sub>*, J. Sichelschmidt, Ph. Schlender, B. Schmidt, M. Baenitz, and Th. Doert, *J. Phys.: Condens. Matter* **31**, (2019) 205601.
- [15]\* *Effective Spin-1/2 Moments on a Yb<sup>3+</sup> Triangular Lattice: an ESR Study*, J. Sichelschmidt, B. Schmidt, Ph. Schlender, S. Khim, Th. Doert, and M. Baenitz, *JPS Conf. Proc.* **30** (2020) 011096.
- [16]\* *Magnetic Properties of an Effective Spin-1/2 Triangular-Lattice Compound LiYbS<sub>2</sub>*, K. M. Ranjith, Ph. Schlender, Th. Doert, and M. Baenitz, *JPS Conf. Proc.* **30** (2020) 011094.
- [17] *Quantum spin liquid ground state in the disorder free triangular lattice NaYbS<sub>2</sub>*, R. Sarkar, Ph. Schlender, V. Grinenko, E. Haeussler, P. J. Baker, Th. Doert, and H.-H. Klauss, *Phys. Rev. B* **100** (2019) 241116(R).
- [18]\* *Tuning of a Kagome Magnet: Insulating Ground State in Ga-Substituted Cu<sub>4</sub>(OH)<sub>6</sub>Cl<sub>2</sub>*, P. Puphal, K. M. Ranjith, A. Pustogow, M. Müller, A. Rogalev, K. Kummer, J. C. Orain, C. Baines, M. Baenitz, M. Dressel, et al., *Phys. Status Solidi B* (2019) 1800663, [doi.org/10.1002/pssb.201800663](https://doi.org/10.1002/pssb.201800663)
- [19] *Theoretical prediction of a strongly correlated Dirac metal*, I. I. Mazin, H. O. Jeschke, F. Lechermann, H. Lee, M. Fink, R. Thomale, and R. Valentí, *Nature Commun.* **5** (2014) 4261.
- [20]\* *Magnetic resonance as a local probe for kagomé magnetism in Barlowite Cu<sub>4</sub>(OH)<sub>6</sub>FBr*, K. M. Ranjith, C. Klein, A. A. Tsirlin, H. Rosner, C. Krellner, and M. Baenitz, *Scientific Reports* **8** (2018) 10851, [doi.org/10.1038/s41598-018-29080-8](https://doi.org/10.1038/s41598-018-29080-8)
- [21]\* *Resonant torsion magnetometry in anisotropic quantum materials*, K. A. Modic, M. D. Bachmann, B. J. Ramshaw, F. Arnold, K. R. Shirer, A. Estry, J. B. Betts, N. J. Ghimire, E. D. Bauer, M. Schmidt, et al., *Nature Communications* **9** (2018) 3975, [doi.org/10.1038/s41467-018-06412-w](https://doi.org/10.1038/s41467-018-06412-w)
- [22]\* *Scale-invariant magnetic anisotropy in RuCl<sub>3</sub> at high magnetic fields*, K. A. Modic, R. D. McDonald, J. P. C. Ruff, M. D. Bachmann, Y. Lai, J. C. Palmstrom, D. Graf, M. K. Chan, F. F. Balakirev, J. B. Betts, et al., *Nature Physics* **17** (2021), [doi.org/10.1038/s41567-020-1028-0](https://doi.org/10.1038/s41567-020-1028-0)

# Michael.Baenitz@cpfs.mpg.de

## Burkhard.Schmidt@cpfs.mpg.de